Available online at www.sciencedirect.com

ScienceDirect

Energy Procedia 50 (2014) 139 – 146

Energy Procedia

The International Conference on Technologies and Materials for Renewable Energy, Environment and Sustainability, TMREES14

Numerical simulation of the type inversion in n+-p-p+ Si solar cells, used for space applications, under 1 MeV electron irradiation

A.Hamache, N. Sengouga* and Af. Meftah

Laboratory of Metallic and Semiconducting Materials (LMSM), Université de Biskra, BP 455 RP, 07000 Biskra, Algeria

Abstract

Solar cells, used for space applications, are exposed to energetic particles such as protons and electrons. The energetic particles create defects in the active region of the solar cell and the latter performance can be severely degraded. One of the phenomenons observed in Silicon solar cells exposed to 1 MeV electron irradiation is type inversion of its active region. This behaviour is numerically simulated using the SCAPS software. The current-voltage characteristics of a Si n+-p-p+ structure are calculated under AM0 for different fluences of 1MeV electrons. It was found that, amongst the many defects created, only one of them is responsible for type inversion. It is a minority trap that is an electron trap in the p-type base of the n+-p-p+ solar cell.

Selection and peer-review under responsibility of the Euro-Mediterranean Institute for Sustainable Development (EUMISD)

Keywords: Si solar cells; 1MeV electron irradiation; type inversion; numerical simulation.

1. Introduction

For terrestrial applications photovoltaic energy is still battling to find a leading place due its relative high cost compared to other sources. However it is the only choice for space applications. Although there is a wide choice of potential materials that can be used to make solar cells, those used to power space vehicles and satellites are required to be highly efficient as well as resistant to energetic particles. The choice then becomes limited to a few materials such as Si and some III-V semiconductors and their all alloys (GaAs, InP and GaInP) [1, 2]. This is mainly due to their mature technology to produce good quality crystals with well controlled doping. Although solar cells made of compound semiconductors have higher conversion efficiencies and radiation-resistance than silicon solar cells, the

*Corresponding author. Tel.: +213 33 54 31 99; fax: +213 33 54 31 99.
E-mail address.n.sengouga@univ-biskra.dz

Selection and peer-review under responsibility of the Euro-Mediterranean Institute for Sustainable Development (EUMISD)
doi:10.1016/j.egypro.2014.06.017

latter have a better cost effectiveness and reliability. The solar cells used in space are subjected to charged particles. The main particles in this environment are protons and electrons of a wide energy range. These interactions introduce defects in the semiconductor lattice and, consequently, deteriorate the solar cell performance [3]. The degradation of solar cells by energetic electrons and protons in laboratories is well documented (see, for example, references [4-8]). In addition to experimental characterisation, analytical modelling is also carried out [9-13]. The main goal of this modelling is to predict the effect of the long term exposure of the solar cells to high energetic electrons and protons [14, 15]. In this modelling the space solar figures of merit (the short circuit current $\boldsymbol{I_{SC}}$, the open circuit voltage $\boldsymbol{V_{OC}}$, the maximum output power $\boldsymbol{P_{MAX}}$, the fill factor $\boldsymbol{FF}$ and the conversion efficiency $\boldsymbol{\eta}$) decreases linearly with the logarithm of the fluence. For example, $\boldsymbol{P_{MAX}}$is related to the irradiation fluence by a simple formula of the form [16]:

$$\boldsymbol{P_{MAX}(\varphi) = P_0\left(1 - C\ln\frac{\varphi}{\varphi_0}\right)} \tag{1}$$

where $\boldsymbol{\varphi}$ is the irradiation fluence, $\boldsymbol{\varphi_0}$ is the fluence threshold for the power reduction, $\boldsymbol{P_0}$ is the pre-irradiated maximum output power and $\boldsymbol{C}$ is a fitting constant. The other figures of merit follow a similar pattern. This analytical modelling is based on the fact that irradiation introduces defects which manifest as energy levels in the semiconductor energy gap and whose concentration is proportional to the fluence, thus:

$$\boldsymbol{N_i = k_i\varphi} \tag{2}$$

The subscript $\boldsymbol{i}$ denotes the $\boldsymbol{i^{th}}$ defect and $\boldsymbol{k_i}$ is introduction rate of the $\boldsymbol{i^{th}}$ defect. It follows that the minority carrier lifetime is reduced, since it is inversely proportional to the defect concentration, as:

$$\boldsymbol{\frac{1}{\tau} = \frac{1}{\tau_0} + \sum\frac{1}{\tau_i} = \frac{1}{\tau_0} + \sum\frac{1}{\tau_i} = \frac{1}{\tau_0} + \sum\sigma_i v_{th}\, N_i = \frac{1}{\tau_0} + \sum\sigma_i v_{th}\, k_i\varphi} \tag{3}$$

$\boldsymbol{\tau_0}$ is the pre-irradiated minority carrier lifetime, $\boldsymbol{\tau_i}$is the minority carrier lifetime set by the $\boldsymbol{i^{th}}$ defect, $\boldsymbol{\sigma_i}$ is the capture cross section of the $\boldsymbol{i^{th}}$ defect and $\boldsymbol{v_{th}}$ is the thermal velocity of minority carriers.

Using (1) it is evident that the solar cell figures of merit decrease monolithically with increasing fluence. However, in some silicon solar cells, the short circuit does not strictly follow this behaviour. Instead, it follows (1) initially and at a certain fluence it increases slightly before it decreases again and sharply [2, 4, 6, 8, 12-13, 17-18]. This slight recovery of the short circuit current is usually attributed to a type inversion of the base silicon (from n to p-type or vice versa) [19]. The type inversion itself is due to the fact that irradiation introduces compensating centres which reduce the initial doping density. As a result the space charge width increases. The phenomenon itself is called carrier removal and is modeled by an analytical expression, for a p-type silicon for example, of the form [2, 13]:

$$\boldsymbol{N_{eff} = N_A - N_{CC} = R_C\varphi} \tag{4}$$

$\boldsymbol{N_{eff}}$ is the effective doping density, $\boldsymbol{N_A}$ is the initial doping density (unirradiated Si), $\boldsymbol{N_{CC}}$ is the compensating centre density and $\boldsymbol{R_C}$ is the removal rate. A more accurate description of the removal phenomenon is described by an exponential behaviour of the reduced hole density [13], thus:

$$\boldsymbol{p_\varphi = p_0 exp\left(-\frac{R_C\varphi}{p_0}\right)} \tag{5}$$

In their detailed analytical modelling, Bourgoin and de Angelis [2] have divided this curve into four regions. Imaizumi et al [4], Yamaguchi et al [6], Yamaguchi et al [13] and Yamaguchi et al [17] have divided the short circuit current dependence on fluence curve into three regions. The first region of [2] is just for $\boldsymbol{\varphi < \varphi_0}$. The other regions are similar between these references. The second region of [2] and the first of the other references is that the short circuit decreases with increasing fluence. This is explained by a decrease in the minority carrier lifetime and hence in their diffusion length. The third region of [2] and the second of the other references is that the short circuit increases with increasing fluence. This is related to the onset of the type inversion where the space charge width increases instead of decreasing. The fourth region of [2] and the third of the other references is that the short circuit falls sharply with increasing fluence. This is explained by the increase in the base resistivity associated with the decrease in carrier concentration. Karazhanov [12] used a straight forward analytical model describing the type inversion using a free concentration compensated by a deep level to explain the increase of the short circuit current with increasing fluence. As it is well known, irradiation creates several defects in semiconductors [1-2, 17, 20-25]. Some of them are recombination centres while others are doping compensating or enhancing centres. In experiment it is very difficult to distinguish between recombination and compensation centres. In addition, analytical modelling links the observed degradation of the solar cell figures of merit to the whole defects. In this respect numerical simulation can be of great help since it can relate the degradation of each figure of merit to a particular defect [26-31]. Of particular interest to the present work, it can reveal which defect is responsible for the type inversion and the anomalous behaviour of the short circuit current in Si solar cells. To accomplish this we have used the software SCAPS (Solar Cell Capacitance Simulator) developed by M. Burgelman and co-workers at the Department of Electronics and Information Systems (ELIS) of the University of Gent, Belgium [32].

2. Simulation

The current-voltage characteristics of the solar cell are calculated using the software SCAPS. SCAPS is a Windows application program, organised in a number of panels, in which the user can set parameters. The program opens with an `action panel', where the user can set an operating point (temperature, voltage, frequency, illumination), and an action list of calculations to carry out (I-V, C-V, C-f, Q(λ)). In each calculation, the running parameter (V, f or λ) is varied in the specified range, whilst all other parameters have the value specified in the operation point. Also, the user can directly view previously calculated results: I-V, C-V, C-f, Q(λ), but also band diagrams, electric field, carrier densities, partial recombination currents.

Like any numerical program, SCAPS solves the basic semiconductor equations. The basic equations are: the Poisson equation, relating the charge to the electrostatic potential ψ, and the continuity equations for electrons and holes. In one dimension, the total cell length L is divided in N intervals, and the value of ψ_i and of the electron and hole concentrationsn_i and p_i at each of the intervals constitute the unknowns of the problem. They can be found by numerically solving 3N non-linear equations, i.e. the basic equations at each of the intervals i. Alternatively, one can choose ψ_i, ϕ_n and ϕ_p as independent variables instead of (ψ_i, n_i, p_i). Here ϕ_n and ϕ_p are the quasi-fermi energy levels for electrons and holes respectively. The basic equations are non-linear because the continuity equations contain a recombination term, which is non-linear in n and p.

The simplest model of charge transport that is useful is the Drift-Diffusion Model. This model is adequate for nearly all devices that were technologically feasible. This model is based on the two first equations cited above. The Poisson's equation which relates the electrostatic potential to the space charge density:

$$div(\varepsilon \nabla \psi) = -\rho \quad (6)$$

where ψ is the electrostatic potential, ε is the local permittivity, and ρ is the local space charge density. The continuity equations for electrons (for example) in steady state, is given by:

$$0 = \frac{1}{q} div \overrightarrow{J_n} + G_n - R_n \quad (7)$$

where n is the electron concentration, $\overrightarrow{J_n}$ is the electron current density, G_n is the generation rate for electrons, R_n is the recombination rate for electrons, and q is the electron charge.

In the drift-diffusion model, the current density is expressed in terms of the quasi-Fermi level ϕ_n as:

$$\vec{J}_n = -q\mu_n n \nabla \phi_n \quad (8)$$

where μ_n is the electron mobility. The quasi-Fermi level is then linked to the carrier concentration and the potential through the Boltzmann approximation:

$$\phi_n = \psi - \frac{k_B T}{q} ln \frac{n}{n_i} \quad (9)$$

where n_i is the effective intrinsic concentration and T is the lattice temperature. By substituting this equation into the current density expression, the current is:

$$\vec{J}_n = qD_n\nabla n - q\mu_n n\nabla\psi - \mu_n n k_B T\nabla ln(n_i) \quad (10)$$

The final term accounts for the gradient in the effective intrinsic carrier concentration, which takes account of bandgap narrowing effects. The conventional formulation of drift-diffusion equation is :

$$\vec{J}_n = qD_n\nabla n + q\mu_n n\vec{E}_n \quad (11)$$

$$\vec{E}_n = -\nabla\psi - \frac{k_B T}{q}\nabla ln(n_i) \quad (12)$$

The electrical characteristics are calculated following the specified physical structure and bias conditions. This is achieved by approximating the operation of the device onto a one dimensional grid, consisting of a number of grid points called nodes. By applying the set of differential equations (Poisson's and continuity equations) onto this grid (discretization), the transport of carriers through the structure can be simulated. The finite element grid is used to represent the simulation domain.

The Si solar cell used in this work is similar to that of [33]. It is a typical 50 µm thick n^+-p-p^+ structure used for space applications. The different parameters of this solar cell are presented in Table 1.

Table 1. The different parameters of the Si solar cell simulated in this work.

	Thickness (µm)	Doping density (cm^{-3})	Type
Emitter	0.15	1×10^{19}	n^+
Base	49.70	1×10^{15}	p
Back surface field region	0.15	5×10^{18}	p^+

.

The I-V characteristics are calculated under AM0 for different fluences of 1MeV electrons. Irradiation by these energetic creates defects in the Si lattice which manifest as recombination centres or traps for free carriers. A lot of work is carried to characterise these defects so that a huge number of defects are detected in Si. For simplicity we have used the most common observed defects [1, 17]. These are summarized in Table 2.

Table 2. The parameters of the defects detected in Si solar cells irradiated by 1 MeV electrons simulated in this work [1, 17]. The trap in these references: hole traps are majority while electron traps are minority in p-type Si. The electron trap $E_C - 0.71$ is only observed in type inverted Si (from p- to n-type).

Activation energy (eV)	Capture cross section, σ (cm^2)	Introduction rate, k (cm^{-1})	Trap type
$E_V + 0.18$	3.1×10^{-15}	0.002	Majority
$E_V + 0.36$	6.2×10^{-15}	0.016	Majority
$E_C - 0.20$	9.9×10^{-15}	0.002	Minority
$E_V + 0.56$	6.3×10^{-13}	0.002	Majority
$E_C - 0.71$	3.55×10^{-13}	0.004	Minority

3. Results and discussions

Since the solar cell used in this work has an n^+-p-p^+ structure, it is expected that the defects will be mainly created within the thickest region which is the p-type base. Therefore the majority traps will only contribute to the reduction of the minority carrier lifetime but not to the type inversion. It is therefore the minority traps which will be responsible for this phenomenon. Referring to table 2, there only two minority traps: $\boldsymbol{E_C - 0.20}$ and $\boldsymbol{E_C - 0.71}$. The second, the deepest, is only observed in type converted Si. In order to establish which trap is responsible for the type inversion we will calculate the I-V characteristics under the effect of each trap. Obviously, the majority traps are taken into account in both cases.

First when only the shallower trap, $\boldsymbol{E_C - 0.20}$, is taken into account, the calculated I-V characteristics under different fluences are shown in Figure 1. It is clear that both the short circuit current and the open circuit voltage decrease with increasing fluence of electron irradiation. However the fill factor (FF) does not change much. The extracted short circuit current normalized to the initial, non irradiated case, is presented in Figure2.

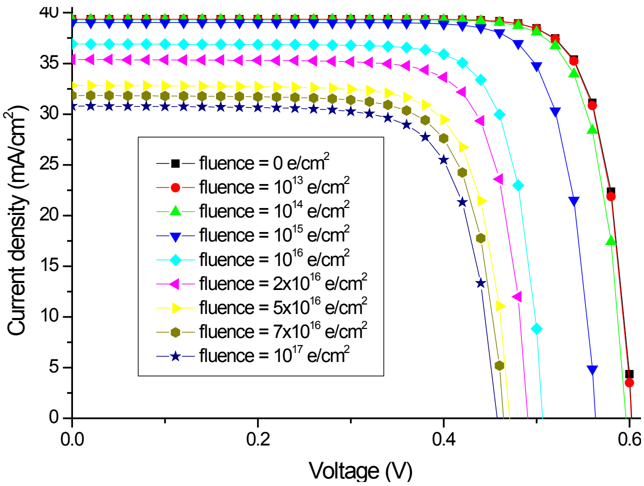

Figure 1. The calculated I-V characteristics of the n+-p-p+ Si solar cell under AM0 for different fluences of 1 MeV electron irradiation taking into account the majority traps and only the shallower minority trap, $E_C - 0.20$.

We can clearly see that the short circuit current decreases monolithically with increasing electron fluence. Therefore the shallower minority trap, $E_C - 0.20$, does not cause the type inversion of the p-type Si base.

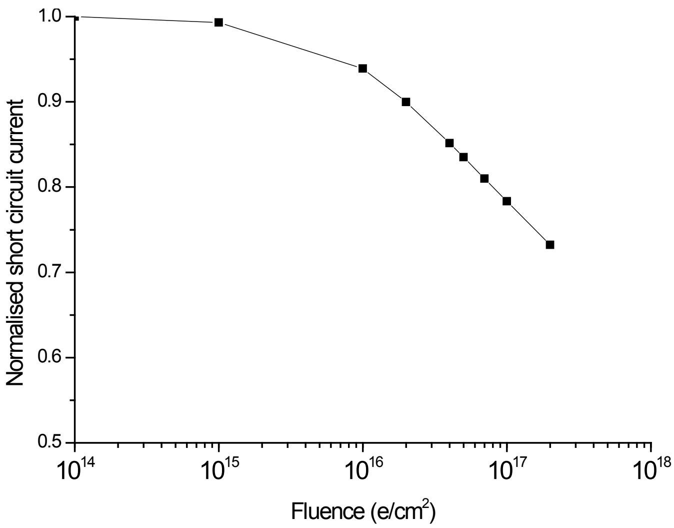

Figure 2. The extracted short circuit current, normalized to the unirradiated value, from the calculated I-V characteristics (Figure 1) of the n+-p-p+ Si solar cell under AM0 for different fluences of 1 MeV electron irradiation taking into account the majority traps and only the shallower minority trap, $E_C - 0.20$.

Next we will consider the effect deeper minority trap, $E_C - 0.71$, on the I-V characteristics of the n+-p-p+ Si solar cell under AM0 for different fluences of 1 MeV electron irradiation. When this trap is taken into account, the calculated I-V characteristics are completely different. These are presented in Figure 3.

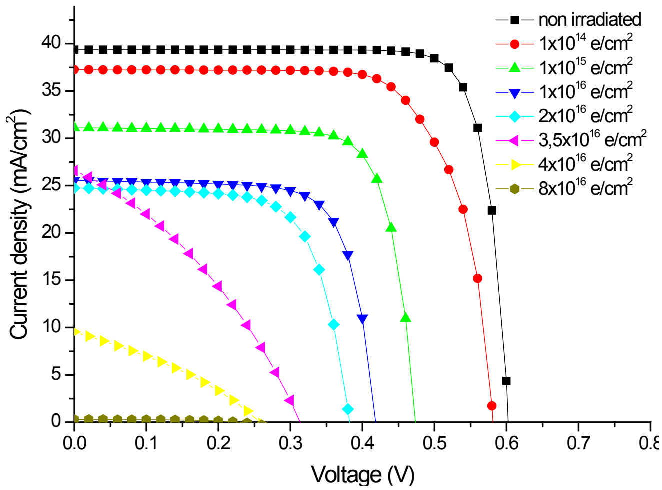

Figure 3. The calculated I-V characteristics of the n+-p-p+ Si solar cell under AM0 for different fluences of 1 MeV electron irradiation taking into account all traps.

It is very clear the big difference from the I-V characteristics of Figure 1. There are two main differences. First the fill factor is hugely affected in contrast to the previous case. Second, the other figures of merit all decrease monolithically with increasing electron fluence except the short circuit current which decreases then increases at a certain fluence before it decreases again and abruptly. This is the type inversion case. To see this phenomenon even clearly, the short circuit current is extracted from the I-V characteristics. It is then normalized to the unirradiated value and presented in Figure 4.

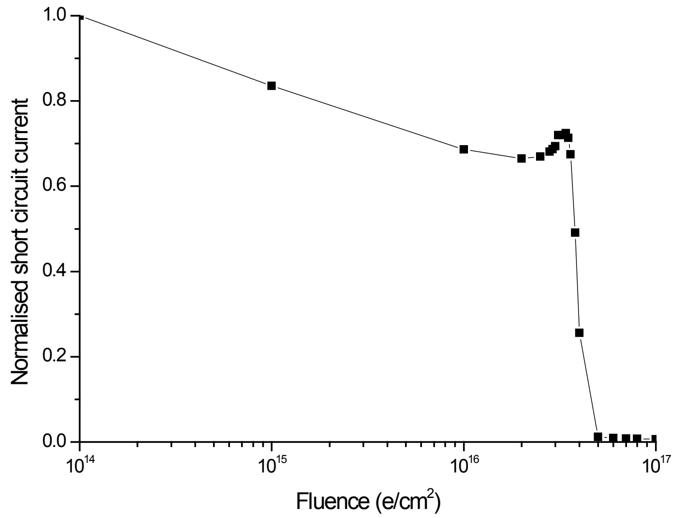

Figure 4. The extracted short circuit current, normalized to the unirradiated value, from the calculated I-V characteristics (Figure 1) of the n+-p-p+ Si solar cell under AM0 for different fluences of 1 MeV electron irradiation taking into account all traps.

In this figure the type inversion phenomenon can be clearly seen. It is also worth to mention that the fluence at which this phenomenon appears is very comparable to measurements of [1, 17]. Although the shallower trap is closer to the conduction band it is less efficient for trapping electrons from the valence band. Therefore it is expected that it will have no effect on the free carrier density. On the other hand the deep minority trap is closed to the valence band therefore it can interchange electrons more easily with the valence band. Since it is a donor, it can give more electrons to the valence band and hence may change Si from p-type to n-type.

4. Conclusion

Numerical simulation using the software SCAPS was carried out to study the effect of 1 MeV electron irradiation of an n+-p-p+ Si solar cell under AM0. Irradiation induces structural defects in the Si lattice. These defects introduce energy levels in the Si forbidden energy gap and which act as recombination centres and/or traps of free carriers. The solar cell performance suffers a sever deterioration as a result. We have concentrated on the type inversion phenomenon which occurs at certain electron fluence. To elucidate this effect, the I-V characteristics where calculated taking into consideration the minority traps separately. It was concluded that the deeper minority trap is responsible for the type inversion phenomenon.

Acknowledgements

We thank Pr. Bulgerman and his colleagues for the use of SCAPS.

References

[1] Masafumi Yamaguchi, Radiation-resistant solar cells for space use, Solar Energy Materials & Solar Cells 68 (2001) 31-53.

[2] J.C. Bourgoin and N. de Angelis, Radiation-induced defects in solar cell materials, Solar Energy Materials & Solar Cells 66 (2001) 467-477.

[3] J.C. Bourgoin, R. Kiliulis, C. Gonzales, G. Strob, C. Flores, K. Bogus and C. Signorini, Deep space degradation of Si and GaAs solar cells, 25th PVSC; May 13-17, 1996; Washington, D.C.

[4] Mitsuru Imaizumi, Stephen J. Taylor, Masafumi Yamaguchi, Tadashi Ito, Tadashi Hisamatsu and Sumio Matsuda, Analysis of structure change of Si solar cells irradiated with high fluence electrons, J. Appl. Phys. 85, 1916 (1999).

[5] B. Danilchenko, A. Budnyk, L. Shpinar, D. Poplavskyy, S.E. Zelensky, K.W.J. Barnham, N.J. Ekins-Daukes, 1MeV electron irradiation influence on GaAs solar cell performance, Solar Energy Materials & Solar Cells 92 (2008) 1336– 1340.

[6] Masafumi Yamaguchi, Stephen J. Taylor, Ming-Ju Yang, Sumio Matsuda, Osamu Kawasaki, and Tadashi Hisamatsu, High-energy and high-fluence proton irradiation effects in silicon solar cells, J. Appl. Phys. 80, 4916 (1996).

[7] Hadrami M, Roubi L, Zazoui M and Bourgoin J C 2006, Relation between solar cell parameters and space degradation, Sol. Energy Mater. Sol. Cells, 90 1486–97

[8] Masafumi Yamaguchi, Aurangzeb Khan, Stephen J. Taylor, Mitsuru Imaizumi, Tadashi Hisamatsu, and Sumio Matsuda, A Detailed Model to Improve the Radiation-Resistance of Si Space Solar Cells, IEEE TRANSACTIONS ON ELECTRON DEVICES, VOL. 46, NO. 10, OCTOBER 1999 2133.

[9] Warner J H, Messenger S R, Walters R J, Summers G P, Lorentzen J R, Wilt D M and Smith M A 2006 Correlation of electron radiation induced-damage in GaAs solar cells, IEEE Trans. Nucl. Sci. 53 1988–94

[10] M. Alurralde, M.J.L. Tamasi, C.J. Bruno, M.G. Martínez Bogado, J. Plá, J. Fernández Vázquez, J. Durán, J. Schuff, A.A. Burlon, P. Stoliar and d, A.J. Kreiner, Experimental and theoretical radiation damage studies on crystalline silicon solar cells, Solar Energy Materials & Solar Cells 82 (2004) 531–542.

[11] S. Makham and G.C.Sun,J.C.Bourgoin, Modelling of solar cell degradation in space, Solar Energy Materials & Solar Cells 94 (2010) 971–978.

[12] S.Zh. Karazhanov, Mechanism for the anomalous degradation of proton- or electron-irradiated silicon solar cells, Solar Energy Materials & Solar Cells 69 (2001) 53-60.

[13] Masafumi Yamaguchi, Stephen J. Taylor, Sumio Matsud and Osamu Kawasaki, Mechanism for the anomalous degradation of Si solar cells induced, by high fluence 1 MeV electron irradiation, Appl. Phys. Lett. 68, 3141 (1996).

[14] S. Makham, M. Zazoui, G.C. Sun, J.C. Bourgoin, Prediction of proton-induced degradation of GaAs space solar cells, Solar Energy Materials & Solar Cells 90 (2006) 1513–1518.

[15] M Mbarki, G C Sun and J C Bourgoin, Prediction of solar cell degradation in space from the electron–proton equivalence, Semicond. Sci.

Technol. 19 (2004) 1081–1085.

[16] R.J. Walters, M.A. Xapsos and G.P. Summers, Radiation response of single and dual junction p+-n InGaP/GaAs space solar cells, Proceedings of the 26th IEEE Photovoltaic Specialist Conference, 29 September–03 October 1997, Anaheim, CA,1997, pp.843–846.

[17] Masafumi Yamaguchi Aurangzeb Khan, Stephen J. Taylor, Koshi Ando and Tsutomu Yamaguchi, Sumio Matsuda and Takashi Aburaya, Deep level analysis of radiation-induced defects in Si crystals and solar cells, J. Appl. Phys. 86, 217 (1999).

[18] N. de Angelis, J.C. Bourgoin, T. Takamoto, A. Khan and M. Yamaguchi, Solar cell degradation by electron irradiation. Comparison between Si, GaAs and GaInP cells, Solar Energy Materials & Solar Cells 66 (2001) 495-500.

[19] Stephen J. Taylor, Masafumi Yamaguchi, Ming-Ju Yang, Mitsuru Imaizumi, Sumio Matsuda, Osamu Kawasaki and Tadashi Hisamatsu, Type conversion in irradiated silicon diodes, Appl. Phys. Lett. 70, 2165 (1997).

[20] Xiang Xianbi, Du Wenhui, Chang Xiulan and Liao Xianbo, Electron irradiation and thermal annealing effect on GaAs solar cells, Solar Energy Materials & Solar Cells 55 (1998) 313-322.

[21] Aurangzeb Khan, Masafumi Yamaguchi, Takashi Aburaya and Sumio Matsuda; Comparison of the effects of electron and proton irradiation on type-converted silicon space solar cells upon annealing, Semicond. Sci. Technol. 15 (2000) 403–407.

[22] C A Londos and P C Banbury, Defect studies in electron-irradiated boron-doped silicon, J. Phys. C: Solid State Phys. 20 (1987) 645-650.

[23] N. Chandrasekaran, T. Soga, Y. Inuzuka, M. Imaizumi, H. Taguchi and T. Jimbo, 1MeV electron irradiation effects of GaAs/Si solar cells, Mater. Res. Soc. Symp. Proc. Vol. 836 (2005), L6.7.1-6.

[24] Aurangzeb Khan, Masafumi Yamaguchi, Tatsuya Takamoto, N. de Angelis and J.C. Bourgoin, Recombination centers in electron irradiated GaInP: application to the degradation of space solar cells, Journal of Crystal Growth 210 (2000) 264-267.

[25] Tadashi Hisamatsu, Sumio Matsuda, Tetsuya Nakao, Yusuke Matsumoto, Stephen J. Taylor and Masafumi Yamaguchi, Thermal recovery of degraded space silicon solar cells due to large fluence irradiation, 26th PVSC; Sept. 30-0ct. 3,1997; Anaheim, CA, 991-4.

[26] A F Meftah, N Sengouga, A Belghachi and A M Meftah, Numerical simulation of the effect of recombination centres and traps created by electron irradiation on the performance degradation of GaAs solar cells, J. Phys.: Condens. Matter 21 (2009) 215802.

[27] A.F. Meftah, N. Sengouga, A.M. Meftah , S. Khelifi, Numerical simulation of the effect of the Al molar fraction and thickness of an $Al_xGa_{1-x}As$ window on the sensitivity of a p^+–n–n^+ GaAs solar cell to 1 MeV electron irradiation,

[28] A.F. Meftah, N. Sengouga, A.M. Meftah, A. Belghachi, Detailed numerical simulation of the effect of defects created by electron irradiation on the performance degradation of a p^+–n–n^+ GaAs solar cell, Renewable Energy 34 (2009) 2422–2425.

[29] AF. Meftah, AM. Meftah, N. Sengouga, S. Khelifi, The $Al_xGa_{1-x}As$ window composition effect on the hardness improvement of a p^+–n–n^+ GaAs solar cell exposed to the electron irradiation, Energy Conversion and Management 51 (2010) 1676–1678.

[30] W. Laiadi, Af. Meftah, N. Sengouga and Am. Meftah, Irradiation effect on the electrical characteristics of an AlGaAs/GaAs based solar cell: Comparison between electron and proton irradiation by numerical simulation, Superlattices and Microstructures 58 (2013) 44–52.

[31] M A Cappelletti, G A Casas, A P Cédola and E L Peltzer y Blancá, Theoretical study of the maximum power point of n-type and p-type crystalline silicon space solar cells, Semicond. Sci. Technol. 28 (2013) 045010.

[32] http://scaps.elis.ugent.be/ See also M. Burgelman, P. Nollet and S. Degrave, Modelling polycrystalline semiconductor solar cells, Thin Solid Films 361-362 (2000) 527-532.

[33] Tadashi Hisamatsu, Osamu Kawasaki, Sumio Matsuda, Tetsuya Nakao and Yoshihito Wakow, Radiation degradation of large fluence irradiated space silicon solar cells, Solar Energy Materials and Solar Cells 50 (1998) 331-338.